AGU PUBLICATIONS

Water Resources Research

RESEARCH ARTICLE

10.1002/2014WR015884

Key Points:
- Isotopic inconsistency between surface and tap water indicates nonlocal water
- Surface and rainwater comparisons form a joint estimate of nonlocal water
- Affluent basins with low surface water availability are likely to import water

Supporting Information:
- tap_water_data.csv
- tap_water_likelihood.py

Correspondence to:
S. P. Good,
s.good@utah.edu

Citation:
Good, S. P., C. D. Kennedy, J. C. Stalker, L. A. Chesson, L. O. Valenzuela, M. M. Beasley, J. R. Ehleringer, and G. J. Bowen (2014), Patterns of local and nonlocal water resource use across the western U.S. determined via stable isotope intercomparisons, *Water Resour. Res.*, *50*, doi:10.1002/2014WR015884.

Received 21 MAY 2014
Accepted 16 SEP 2014
Accepted article online 12 SEP 2014

Patterns of local and nonlocal water resource use across the western U.S. determined via stable isotope intercomparisons

Stephen P. Good[1], Casey D. Kennedy[2], Jeremy C. Stalker[3], Lesley A. Chesson[4], Luciano O. Valenzuela[5,6], Melanie M. Beasley[7], James R. Ehleringer[6], and Gabriel. J. Bowen[1]

[1]Department of Geology and Geophysics, University of Utah, Salt Lake City, Utah, USA, [2]United States Department of Agriculture, Agricultural Research Service, East Wareham, Massachusetts, USA, [3]Biology and Marine Science, Jacksonville University, Jacksonville, Florida, USA, [4]IsoForensics Inc., Salt Lake City, Utah, USA, [5]Consejo Nacional de Investigaciones Cientficas y Tcnicas, Laboratorio de Ecologa Evolutiva Humana, UEUQ-UNCPBA, Buenos Aires, Argentina, [6]Department of Biology, University of Utah, Salt Lake City, Utah, USA, [7]Department of Anthropology, University of California, San Diego, San Diego, California, USA

Abstract In the western U.S., the mismatch between public water demands and natural water availability necessitates large interbasin transfers of water as well as groundwater mining of fossil aquifers. Here we identify probable situations of nonlocal water use in both space and time based on isotopic comparisons between tap waters and potential water resources within hydrologic basins. Our approach, which considers evaporative enrichment of heavy isotopes during storage and distribution, is used to determine the likelihood of local origin for 612 tap water samples collected from across the western U.S. We find that 64% of samples are isotopically distinct from precipitation falling within the local hydrologic basin, a proxy for groundwater with modern recharge, and 31% of samples are isotopically distinct from estimated surface water found within the local basin. Those samples inconsistent with local water sources, which we suggest are likely derived from water imported from other basins or extracted from fossil aquifers, are primarily clustered in southern California, the San Francisco Bay area, and central Arizona. Our isotope-based estimates of nonlocal water use are correlated with both hydrogeomorphic and socioeconomic properties of basins, suggesting that these factors exert a predictable influence on the likelihood that nonlocal waters are used to supply tap water. We use these basin properties to develop a regional model of nonlocal water resource use that predicts ($r^2 = 0.64$) isotopically inferred patterns and allows assessment of total interbasin transfer and/or fossil aquifer extraction volumes across the western U.S.

1. Introduction

Expanding human populations and agricultural production threaten human water security by creating large water resources demands beyond of the supply capacity of local regions [*Vörösmarty et al.*, 2010]. In order to successfully meet rising demands, management approaches must be sustainable in the long term, and interbasin water transfer projects are one approach used to meet growing water resource requirements [*Ghassemi and White*, 2007]. Within the U.S., an estimated 5.8 trillion gallons (22 billion cubic meters) of water were transferred per year during the 1973–1982 period [*Buckley*, 2013] based on the most recent federal surveys of 256 water transfer projects in the eastern [*Mooty and Jeffcoat*, 1986] and western [*Petsch*, 1985] U.S. The largest exporters of water in the U.S. are the lower Colorado River region and the Sacramento River delta area, which move water to the large population centers of southern California and the San Francisco Bay area [*Buckley*, 2013]. Beyond these two large transfer schemes, a wide variety of local, state, and federal projects are currently in operation or planned (Figure 1).

In addition to interbasin water transfers, many regions suffering under high water demands have resorted to the pumping of groundwater resources [*Sultan et al.*, 2007]. In the U.S., several aquifer systems are being rapidly depleted (Figure 1), and the cumulative volume of groundwater depletion in the 20th century is estimated at ~211 trillion gallons (800 billion cubic meters), with the largest depletions occurring in the High Plains aquifer, the Mississippi embayment aquifer system, and the Central Valley aquifer system of California [*Konikow*, 2013]. Over the long term as groundwater is extracted from aquifers, decreased discharge and/or

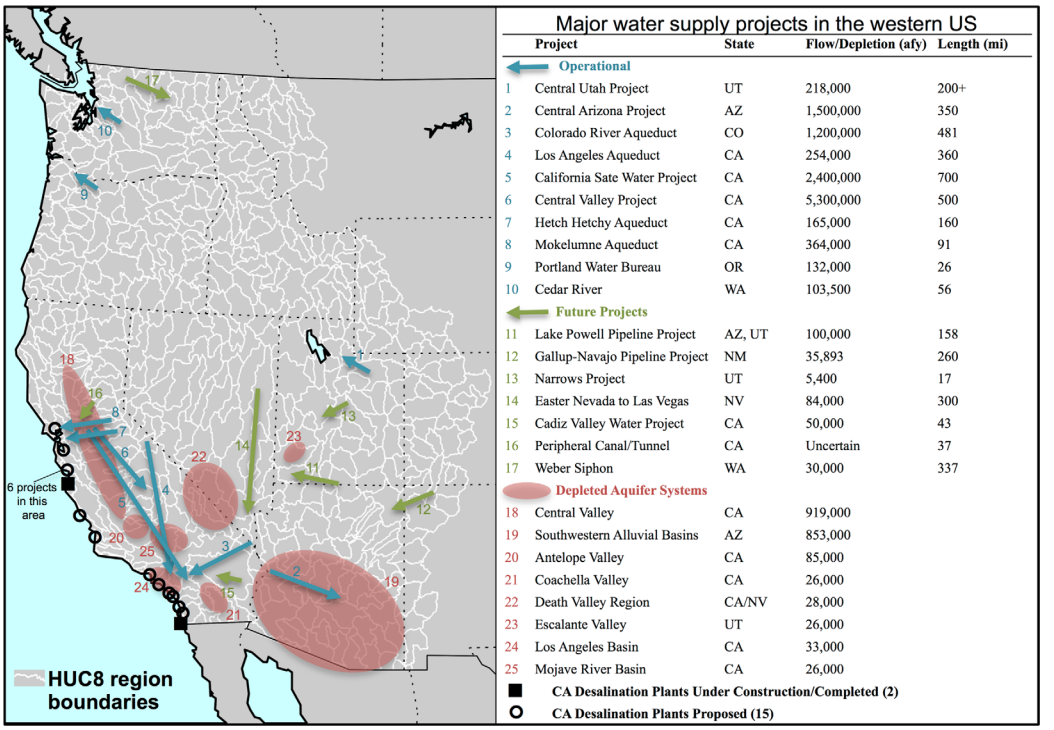

Figure 1. Selected major water transfer projects in the western U.S. Data and map are adapted from *Fort et al.* [2012] and *Konikow* [2013]. Locations are approximate, flows and average depletions (1900–2000) for aquifers are expressed in acre-feet per year (afy) and lengths are in miles (mi). California desalination facility information adapted from *Cooley and Donnelly* [2012]. White lines denote USGS hydrologic basins (HUC8) west of the continental divide within the U.S.

increased recharge leads toward an equilibrium point, however, in the case of fossil aquifers where modern recharge is unavailable, extractions constitute permanent groundwater mining [*Konikow and Kendy*, 2005]. The permanent depletion of groundwater resources not only impacts water supply, but can result in land subsidence, reductions in surface flows, and wetlands loss [*Konikow*, 2013]. Though the majority (77%) of water withdrawals in the U.S. are from surface water sources, many Western states use less surface water (e.g., California—67%; Arizona—51%, New Mexico—49%) and more groundwater than the national average [*Kenny et al.*, 2009]. Furthermore, in the state of California, a number of desalination facilities are proposed and under construction, including the 50 million gallon per day project by the San Diego Water Authority scheduled to begin water distribution in 2014 [*Cooley and Donnelly*, 2012]. With expanding demands and a changing climate, interbasin transfers, groundwater pumping, and in some cases desalination, are increasingly looked to as a solution to alleviate water deficits throughout the west [*Fort et al.*, 2012].

The grand scale and massive funding required to implement water infrastructure projects results in a rigidity in water resource management options [*Gupta and van der Zaag*, 2008] and complicates the economics of water supply networks and their optimization [*Draper et al.*, 2003; *Jenkins et al.*, 2004]. Alterations to the connectivity and flow regimes of natural hydrologic systems have implications for the biodiversity and biogeography of riverine communities [*Lynch et al.*, 2011; *Grant et al.*, 2012; *Yan et al.*, 2012]. Given the hydrologic, economic, and biological consequences of nonlocal water use, it is important to quantify patterns in interbasin transfers and fossil groundwater mining, and to identify the characteristics of watersheds that require alternate supply of water resources. However, the last federal inventories of water transfer projects in the U.S. were completed in 1985 and 1986 by the U.S. Geologic Survey [*Petsch*, 1985; *Mooty and Jeffcoat*, 1986], and an updated assessment is required. Furthermore, changes to and expansions of water transfer networks combined with increased security concerns in recent years complicate the direct compilation of all local, state, and federal projects into a national database. Calculation of groundwater depletions also suffers from limited reliability as various estimation methods (water-level change, gravity measurements, flow modeling, confining unit assessment,

pumpage fraction, and subsidence monitoring) have accuracies ranging from less than 1%–40% of measured depletion values [*Konikow*, 2013], and distinguishing between fossil groundwater mining and withdraws from aquifers recharged with modern precipitation remains a challenge. Finally, assessing the impact of large water projects on developing regions such as in China [*Yan et al*., 2012], India [*Lynch et al*., 2011], and Egypt [*Sultan et al*., 2007] requires investigative strategies not dependent on detailed knowledge of local water supply infrastructure layout or operation.

An alternative approach to directly compiling data from the large variety of water transfer projects and fossil groundwater extractions across the U.S. is to use geochemical tracers to compare supplied waters (i.e., tap waters) with local water resources. As vapor is transported through global atmospheric processes, moist air masses become more enriched in heavy isotopes of oxygen (δ^{18}O) and hydrogen (δ^{2}H) as a result of progressive condensation coupled with liquid-vapor fractionation during rainout [*Craig*, 1961; *Dansgaard*, 1964]. Atmospheric distillation of heavy isotopes results in temperature, altitude, and latitude-dependent gradients in precipitation isotopic ratios and since the 1960s groups such as the Global Network of Isotopes in Precipitation (GNIP) have collected precipitation to characterize spatial patterns in isotope ratios [*Rozanski et al*., 1993; *Vachon et al*., 2010]. Additional studies have investigated spatial precipitation isotope patterns during specific large-scale rainfall events [*Gedzelman and Lawrence*, 1990; *Good et al*., 2014] and how atmospheric trajectories influence precipitation isotopic composition [*Soderberg et al*., 2013; *Brown et al*., 2013]. Further studies have extended spatial characterizations of isotope ratios to surface waters throughout the U.S. [*Kendall and Coplen*, 2001; *Bowen et al*., 2011].

Groundwater recharged with modern precipitation is likely to have isotopic compositions similar to local or regional precipitation and surface water, and its spatial pattern can be inferred by using precipitation as a proxy [*Gat*, 1996; *Smith et al*., 2002; *Bowen et al*., 2012]. However, in previous geologic periods such as the Pleistocene, cooler temperatures resulted in isotopically lighter precipitation, and fossil groundwater recharged during such times is likely to be isotopically distinct from modern sources at the same site [*Smith et al*., 2002]. Stable isotope tracers have therefore served as an indicator of paleo-waters throughout the world [*Sultan et al*., 2007; *Smith et al*., 2002]. Given these factors, divergence in stable isotope values can best be viewed as indicative of situations where tap water is derived from water resources that are separated from contemporary local waters in space (i.e., interbasin transfer) or time (i.e., recharge under different conditions in the past), and thus as facilitating assessment of anthropogenically altered hydrologic conditions at the regional scale [*Williams and Rodoni*, 1997].

Across the U.S., coherent patterns have been found in the tap water isotopic composition, and large isotopic discrepancies between local water resources and supplied tap water signify that supplied waters may be derived from interbasin transfers or fossil groundwaters [*Bowen et al*., 2007; *Landwehr et al*., 2013]. The first national-scale maps of δ^{2}H and δ^{18}O values in tap waters were presented by *Bowen et al*. [2007], and more recently, *Landwehr et al*. [2013] conducted a second detailed study of U.S. tap waters. These studies identified clear inconsistencies between tap waters and local surface waters, with distinct spatial patterns. Similarly, *Chesson et al*. [2010] analyzed bottled waters from around the U.S. and found that region of origin information is recorded in isotopic composition of these waters. The isotopic signature of consumed waters is also transferred into plant and human tissues [*Kelly et al*., 2005; *Ehleringer et al*., 2008], and understanding the connection between tap water isotope ratios and geographic location has additional potential for application in the burgeoning field of isotope forensics [*Beasley et al*., 2013].

The objective of this paper is to evaluate the use of stable isotope tracers to distinguish between local and nonlocal water sources. Previously, this type of comparison has been significantly hindered by the possibility that samples have been isotopically altered by processes such as evaporation. Here we present a new methodology that considers both the potential for evaporative enrichment during storage and distribution of waters in public networks as well as uncertainty in tap water and hypothesized local source water isotopic values to provide a quantitative assessment of the likelihood of local origin. We use this method to evaluate the likelihood of local water origin for a suite of 612 tap water samples from the western U.S. The estimated likelihoods are then compared to local hydrogeomorphic and socioeconomic factors including basin size, elevation, temperature, relative humidity, rainfall, outflow, population density, income, and water availability. A multivariate regression model developed based on these local characteristics is used to predict the likelihood of local water use in locations where tap water samples have not been collected. Finally, our results are used to assess regional patterns in water supply throughout the western U.S.

2. Methodology

2.1. Data Sources

The database of tap water isotope ratios (included as supplementary materials: tap_water_data.csv) was compiled from previously published studies by *Bowen et al.* [2007] and *Kennedy et al.* [2011] as well as newly collected samples. Samples were collected between 2002 and August 2003 [*Bowen et al.*, 2007; *Kennedy et al.*, 2011] with additional samples collected during the fall of 2010 and summer of 2011 and 2012. Water samples were collected from faucets in domestic and commercial buildings by running cold tap water for ~10 s before filling, capping, and sealing with parafilm, a clean two dram vial. Samples were analyzed at the Stable Isotope Ratio Facility for Environmental Research (SIRFER) at the University of Utah and the Purdue Stable Isotope (PSI) laboratory at Purdue University.

Analysis of samples was conducted via dual inlet isotope ratio mass spectrometry [*Bowen et al.*, 2007; *Kennedy et al.*, 2011] and continuous flow isotope ratio mass spectrometry [*Kennedy et al.*, 2011] (IRMS: Delta +XL, ThermoFinnigan), as well as wavelength-scanned cavity ring-down spectroscopy (CRDS: L-1102-i, Piccaro Inc.). Oxygen and hydrogen isotopic composition are expressed in δ notation, $\delta = (R/R_{std} - 1)$, where R is the ratio of rare to abundant isotopes and R_{std} refers to the same ratio in Vienna Standard Mean Ocean Water (VSMOW) [*De Laeter et al.*, 2003]. All δ values are reported in permil (‰) notation, which is equivalent to 1×10^3 [*Coplen*, 2011]. All sample values were normalized on the VSMOW-VSLAP standard scale. IRMS samples were analyzed in duplicate, and CRDS samples were injected four times to compensate for memory effects, with only the last two injections considered. Samples were calibrated with two working standards [*Coplen*, 1996], with an average precision of 1.5‰ for δ^2H and 0.2‰ for δ^{18}O (1σ) for replicate analyses.

Each collected tap water is assumed to be drawn from a sample distribution $\mathbf{d}_s = [\mathbf{m}_s, \mathbf{S}_s]$, characterized by a mean ($\mathbf{m}_s$) and covariance matrix ($\mathbf{S}_s$) as

$$\mathbf{m}_s = \begin{bmatrix} \mu_{(\delta^{18}\mathrm{O})_s} & \mu_{(\delta^2\mathrm{H})_s} \end{bmatrix}, \tag{1a}$$

$$\mathbf{S}_s = \begin{bmatrix} \sigma^2_{(\delta^{18}\mathrm{O})_s} & 0 \\ 0 & \sigma^2_{(\delta^2\mathrm{H})_s} \end{bmatrix}. \tag{1b}$$

The measured δ^{18}O value, $\mu_{(\delta^{18}\mathrm{O})_s}$, with analytical uncertainty $\sigma_{(\delta^{18}\mathrm{O})_s}$ and the measured δ^2H value, $\mu_{(\delta^2\mathrm{H})_s}$, with analytical uncertainty $\sigma_{(\delta^2\mathrm{H})_s}$ are treated as independent variables. Values of $\sigma_{(\delta^{18}\mathrm{O})_s}$ and $\sigma_{(\delta^2\mathrm{H})_s}$ were fixed at 0.2‰ and 1.5‰, respectively, for all samples based on the average uncertainty of the IRMS analysis. The 612 water samples collected from Arizona, California, Idaho, Nevada, Oregon, Utah, and Washington used in this study (Figure 2) span a range of −18.9‰ to −1.1‰ for δ^{18}O and −145.4‰ to −8.3‰ for δ^2H. As presented here, our approach tests whether each sample distribution is consistent with the isotopic distributions found within the local basin but does not consider seasonality or correlation within a given tap water sample distribution and therefore does not require multiple samples or the characterization of long-term variability in supplied waters. Variability within each basin is captured by the local water distribution of rainfall and surface waters against which sample distributions are compared.

The spatial pattern of precipitation isotope values (Figure 3a) was estimated based on data collected by the Global Network of Isotopes in Precipitation (GNIP) and other groups as presented in *Bowen and Wilkinson* [2002] and *Bowen and Revenaugh* [2003]. This approach treats the isotopic composition of precipitation as the sum of temperature-driven rainout effects and regional patterns of vapor sourcing and delivery. Rainout effects are represented through model parameters relating isotopic composition at measurement stations to latitude and altitude. Regional variation due to atmospheric circulation patterns is included though spatial interpolation of isotopic variability not accounted for in the rainout model. The final results of this approach are global maps of δ^{18}O and δ^2H isotopic composition at fine spatial resolution (5′ by 5′ over land and 20′ by 20′ over ocean) that are precipitation amount weighted to give the annual isotopic composition at each point. Uncertainties are assessed via a Jackknifing approach [*Wu*, 1986], giving global maps of prediction uncertainty with averages of ~9.4‰ for δ^2H and 1.17‰ δ^{18}O (2σ). At each grid cell, uncertainty is estimated based on that cell's properties (latitude, elevation, temperature) as well as the distance to stations where precipitation was collected for isotope measurements.

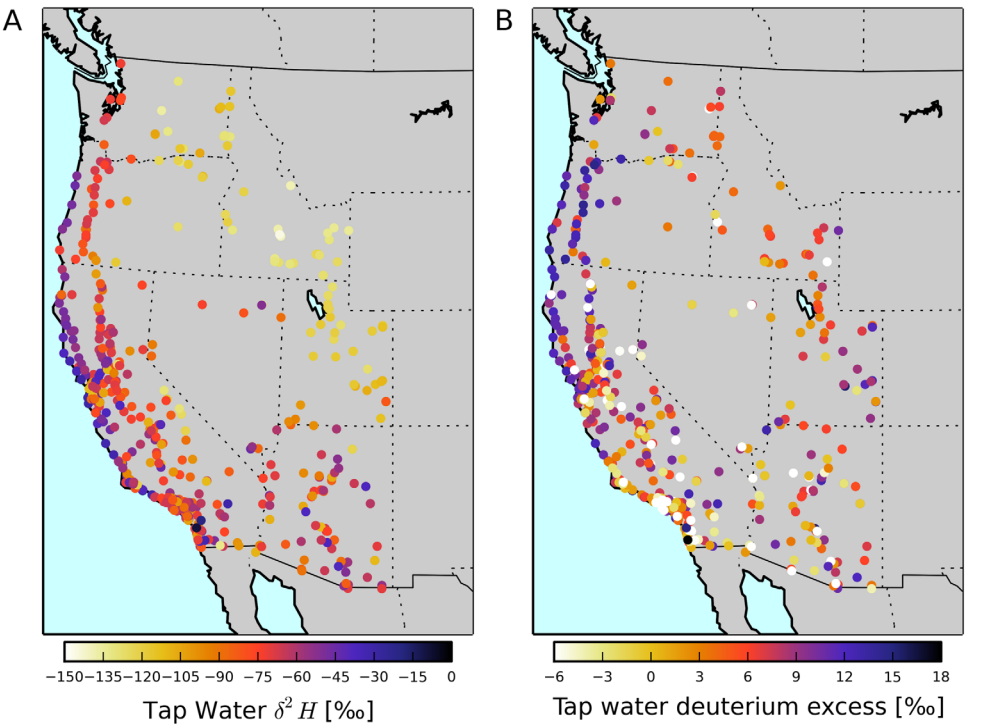

Figure 2. Collected tap water (a) δ^2H isotopic composition and (b) deuterium excess.

The isotopic compositions of surface waters (Figure 3b) were estimated based on the results of the spatiotemporal surface water isotope balance of *Bowen et al*. [2011]. This approach routes surface water flows within a 1 km gridded digital elevation model considering both precipitation and evaporation fluxes within each cell. Isotopic compositions were then estimated as the mass weighted sum of upstream contributions. The final data set was then bias corrected based on the surface water samples of *Kendall and Coplen* [2001] with a final cross-validation root mean square errors of 9.2‰ and 1.3‰ for δ^2H and δ^{18}O, respectively. Similar to the precipitation fields, the surface water fields are spatiotemporaly flow weighted such that the isotopic composition is the annual average at each point and uncertainty is determined separately for each grid cell.

Where water is stored in reservoirs or during its distribution though open-air supply networks, evaporation is likely to occur. During evaporation, the light isotopes of H and O are preferentially lost and kinetic fractionation alters δ^{18}O and δ^2H. Thus as a water body evaporates, the remaining liquid becomes enriched in heavier isotopes along a local evaporation line with an average slope that differs from that of the global meteoric water line [*Gibson et al*., 2008]. We define the local evaporation line, $g(t)$, as the function that gives the δ^2H isotopic composition for a δ^{18}O value of t as

$$g(t|x_l, y_l, x_*, y_*) = \left(\frac{y_* - y_l}{x_* - x_l}\right)(t - x_l) + y_l, \tag{2}$$

where x_l and y_l are the δ^{18}O and δ^2H isotopic composition of a local water source. The values, x_* and y_*, are the steady state δ^{18}O and δ^2H isotopic composition of an evaporating body of water under local climatological conditions and calculated as $\delta_* = \varepsilon/h + \delta_A$, where ε is the limiting isotopic enrichment (including equilibrium and kinetic effects), h is the relative humidity, and δ_A is the atmospheric composition of atmospheric vapor (assumed in equilibrium with local precipitation) [*Gat and Levy*, 1978; *Gibson and Edwards*, 2002]. Note that the first term in parentheses on the right-hand side of equation (2) is the local evaporation slope. Local meteorological conditions were estimated based on data from the PRISM climate group [*Daly et al*., 2002]. Without direct knowledge of source composition for a given sample, it is impossible to know the degree of δ^{18}O evaporative enrichment, (i.e., $t - x_l$), along the line

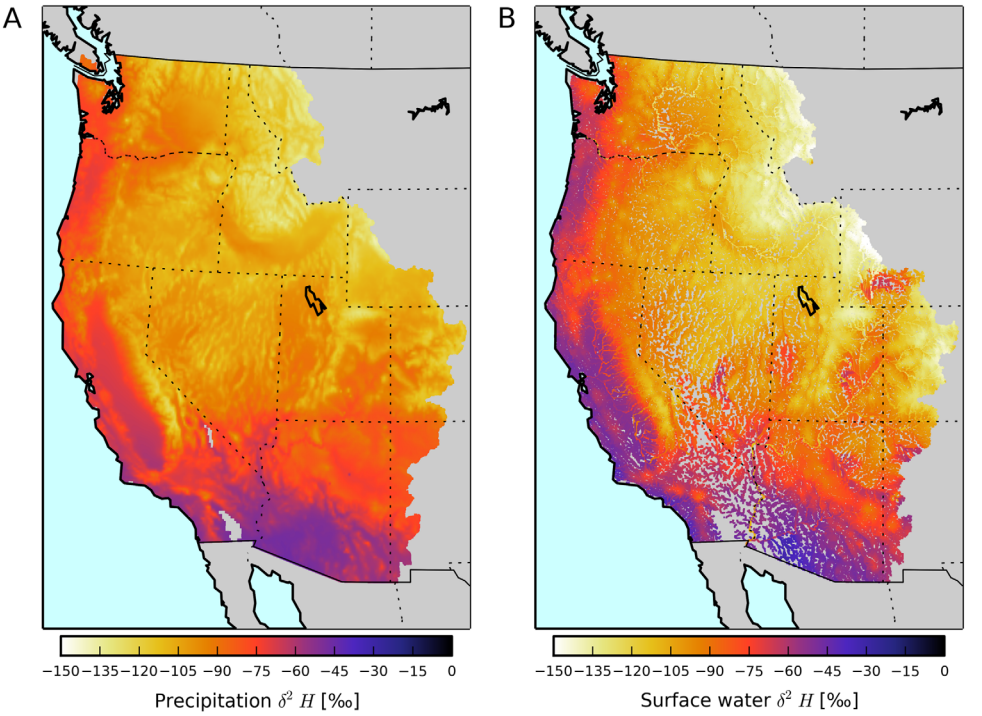

Figure 3. Estimated δ^2H isotopic composition in (a) precipitation and (b) surfaces waters.

described in equation (2), and therefore only points where $x_l < t < x_*$ are assumed as possible final enriched values.

For this analysis, we define local water as the weighted average precipitation or surface water within each eight-digit hydrologic unit of the U.S. National Watershed Boundary Dataset (http://datagateway.nrcs.usda.gov). The national Watershed Boundary Dataset Hydrologic Unit Code 8 digit (HUC8) classification is used to define the local hydrologic basin extent (Figure 1: HUC8 units 14000000–18000000). The HUC8 layer delineates the U.S. and hydrologically connected regions in Canada and Mexico into 2149 basins, where each basin has an average area of 700 mi^2 [*USGS*, 2013]. This area is approximately equal to a circular region with a 15 mi radius. The HUC8 boundaries, as opposed to a circular distance buffer around each sample location, are used in order to ensure that local waters do not include isotopic values that fall beyond a watershed divide. Comparisons of tap waters are made with the average basin isotopic composition, independent of sample location within a basin. HUC8 delineation of local waters corresponds to the water resource areas relevant to interbasin water transfers and served as the reference unit for previous investigations [*Mooty and Jeffcoat*, 1986; *Petsch*, 1985; *Buckley*, 2013]. Note, that a transfer downstream within the same macrowatershed from one HUC8 region to another (as in the case of transfers from the Sierra Nevada mountains to San Francisco) is still considered an interbasin transfer in this framework; however, our methodology here is not likely to identify this type of transfer because water artificially diverted in this manner is anticipated to be similar to the surface water values of major rivers linking these areas. Data on the population and average household income within each HUC8 region were obtained from the Topologically Integrated Geographic Encoding and Referencing (TIGER) data sets produced by the U.S. Census Bureau (http://www.census.gov/geo/maps-data/data/tiger.html [*Census*, 2013]) and aggregated to the national level by NASA's Socioeconomic Data Application Center (SEDAC) [*Seirup and Yetman*, 2006].

Source waters available in each basin are assumed to be drawn from a local distribution $\mathbf{d}_l = [\mathbf{m}_l, \mathbf{S}_l]$, characterized by a mean ($\mathbf{m}_l$) and covariance matrix ($\mathbf{S}_l$) as

$$\mathbf{m}_l = \left[\mu_{(\delta^{18}\mathrm{O})_b} \quad \mu_{(\delta^2\mathrm{H})_b} \quad \mu_{(\delta^{18}\mathrm{O})_*} \quad \mu_{(\delta^2\mathrm{H})_*} \right], \tag{3a}$$

$$\mathbf{S}_l = \begin{bmatrix} \sigma^2_{(\delta^{18}\mathrm{O})_b} + \sigma^2_{(\delta^{18}\mathrm{O})_i} & \sigma_{(\delta^{18}\mathrm{O},\delta^2\mathrm{H})_b} + \sigma_{(\delta^{18}\mathrm{O},\delta^2\mathrm{H})_i} & 0 & 0 \\ \sigma_{(\delta^{18}\mathrm{O},\delta^2\mathrm{H})_b} + \sigma_{(\delta^{18}\mathrm{O},\delta^2\mathrm{H})_i} & \sigma^2_{(\delta^2\mathrm{H})_b} + \sigma^2_{(\delta^2\mathrm{H})_i} & 0 & 0 \\ 0 & 0 & \sigma^2_{(\delta^{18}\mathrm{O})_*} & \sigma_{(\delta^{18}\mathrm{O},\delta^2\mathrm{H})_*} \\ 0 & 0 & \sigma_{(\delta^{18}\mathrm{O},\delta^2\mathrm{H})_*} & \sigma^2_{(\delta^2\mathrm{H})_*} \end{bmatrix}. \tag{3b}$$

For both the precipitation and surface water sources, we estimate the parameters of the distribution $\mathbf{d}_l$ based on the weighted mean and standard deviation of values within each hydrologic basin. For local precipitation, the rainfall amount weighted average of the precipitation isotopic composition and the rainfall amount weighted standard deviation are calculated for each hydrologic basin. Similarly, for local surface waters, weighting is done based on calculated flows at each grid cell within the basin. The average basin δ^{18}O value, $\mu_{(\delta^{18}\mathrm{O})_b}$, with within-basin variability $\sigma_{(\delta^{18}\mathrm{O})_b}$ and the average basin δ^2H value, $\mu_{(\delta^2\mathrm{H})_l}$, with within-basin variability $\sigma_{(\delta^2\mathrm{H})_b}$ are treated as variables with known covariance $\sigma_{(\delta^{18}\mathrm{O}_b,\delta^2\mathrm{H}_b)}$, where $\sigma_{(\delta^{18}\mathrm{O}_b,\delta^2\mathrm{H}_b)}$ is the covariance of values from all grid cells within the basin. Additionally, the rainfall interpolation or surface water model uncertainty ($\sigma_{(\delta^{18}\mathrm{O})_i}$, $\sigma_{(\delta^2\mathrm{H})_i}$) and its associated covariance are added to the local covariance matrix $\mathbf{S}_l$. The steady state evaporation isotopic composition ($\mu_{(\delta^{18}\mathrm{O})_*}$, $\mu_{(\delta^2\mathrm{H})_*}$) and its associated uncertainty ($\sigma_{(\delta^{18}\mathrm{O})_*}$, $\sigma_{(\delta^2\mathrm{H})_*}$, $\sigma_{(\delta^{18}\mathrm{O},\delta^2\mathrm{H})_*}$) are treated as independent of the local source water. Although both precipitation and surface waters are amount weighted based on seasonality, we do not explicitly consider the inter-seasonal variability in isotopic composition in the covariance matrix $\mathbf{d}_l$; therefore, our approach only assesses the likelihood that a tap water sample is consistent with the mean isotopic composition in a basin. However, spatial variability in isotopic composition within individual HUC8 regions can be quite large and significantly exceed the temporal variability in the basin average composition, this is especially true in basins with large elevational gradients where altitude effects are significant.

2.2. Likelihood Assessment

The relative likelihood that a given water sample is of local origin, $\mathcal{L}_r$, is assessed through a Bayesian approach modified from *Kennedy et al.* [2011]. The posterior distribution, $P(\mathbf{d}_l|\mathbf{d}_s)$, expresses the probability that a basin having an estimated isotopic distribution of local precipitation or surface water ($\mathbf{d}_l$) served as the origin of collected tap water with a sample distribution ($\mathbf{d}_s$) and is defined by Bayes rule as

$$P(\mathbf{d}_l|\mathbf{d}_s) = \frac{P(\mathbf{d}_s|\mathbf{d}_l)P(\mathbf{d}_l)}{\int P(\mathbf{d}_s|\mathbf{d}_l)P(\mathbf{d}_l)}. \tag{4}$$

The prior probability distribution, $P(\mathbf{d}_l)$, defines the probability that a local source water will occur within each HUC8 region. Finally, the conditional probability $P(\mathbf{d}_s|\mathbf{d}_l)$ is the likelihood of obtaining the sample with distribution $\mathbf{d}_s$ given the local source water distribution $\mathbf{d}_l$ [*Wunder et al.*, 2005; *Wunder*, 2010; *Kennedy et al.*, 2011].

Here $P(\mathbf{d}_s|\mathbf{d}_l)$ is evaluated using a new algorithm that integrates the sample distribution, $f_{\mathbf{d}_s}$, along possible evaporation lines, $g(t)$. The value of $P(\mathbf{d}_s|\mathbf{d}_l)$ is calculated by multiplying these integrated values by the probability of a specific evaporation line occurring, $f_{\mathbf{d}_l}$. This is expressed as

$$P(\mathbf{d}_s|\mathbf{d}_l) = \iiiint_{\mathbb{R}^4} f_{\mathbf{d}_l}(x_l, y_l, x_*, y_*) \int_{x_l}^{x_*} g'(t)\, f_{\mathbf{d}_s}(t, g(t))\, dt\, dx_l\, dy_l\, dx_*\, dy_*. \tag{5}$$

where $f_{\mathbf{d}}(\mathbf{x})$ is assumed to be the standard multivariate normal distribution with mean $\mathbf{m}$ and covariance matrix $\mathbf{S}$ evaluated at $\mathbf{x}=x_1, \ldots, x_k$, as given by

$$f_{\mathbf{d}_i}(\mathbf{x}) = \frac{1}{\sqrt{(2\pi)^k|\mathbf{S}|}} \exp\left(-\frac{1}{2}(\mathbf{x}-\mathbf{m})^T\mathbf{S}^{-1}(\mathbf{x}-\mathbf{m})\right). \tag{6}$$

The approach in equation (5) examines all possible evaporative enrichments (t integrated from x_l to x_*) along evaporation lines with all possible local source and steady state endpoints (x_l, y_l and x_*, y_* integrated from $-\infty$ to ∞ in $\mathbb{R}^4$) and their probability of occurring ($f_{\mathbf{d}_l}$) against the probability of a given value of the source water occurring ($f_{\mathbf{d}_s}$). Equation (5) is a presented in a general form such that once the local ($f_{\mathbf{d}_l}$) and

sample ($f_{\mathbf{d}_s}$) probability distribution are specified, any form of isotopic transformation can be used by formulating $g(t)$ to match the isotopic change expected. The first derivative of the local evaporation line, $g'(t)$, is required to properly evaluate the line integral with respect to δ^{18}O composition.

In practice, equation (5) can be evaluated numerically over a large number, n, of random realizations of the local source water as

$$P(\mathbf{d}_s|\mathbf{d}_l) \approx \sum_{j=1}^{n} \frac{1}{n} \sum_{t=x_j}^{x_*} \frac{\Delta t \sqrt{1+\left(\frac{{}^{j}y_* - {}^{j}y_l}{{}^{j}x_* - {}^{j}x_l}\right)^2}}{2\pi\sigma_{(\delta^{18}\mathrm{O})_s}\sigma_{(\delta^{2}\mathrm{H})_s}} \exp\left(-\frac{(t-\mu_{(\delta^{18}\mathrm{O})_s})^2}{2\sigma^2_{(\delta^{18}\mathrm{O})_s}} - \frac{\left(\left(\frac{{}^{j}y_* - {}^{j}y_l}{{}^{j}x_* - {}^{j}x_l}\right)(t-x_j)+y_j-\mu_{(\delta^{2}\mathrm{H})_s}\right)^2}{2\sigma^2_{(\delta^{2}\mathrm{H})_s}}\right). \quad (7)$$

where ${}^{j}x_l$, ${}^{j}y_l$, ${}^{j}x_*$, and ${}^{j}y_*$ are the jth random realizations of local source and steady state water drawn from $\mathbf{d}_l$. Δt is chosen to be a small interval, e.g., $\sigma_{(\delta^{18}\mathrm{O})_s}/10$, such that the Riemann sum is a sufficient approximation of the inner integral in equation (5). Evaluation of equation (7) is preformed with a Python script (included as supplementary materials: tap_water_likelihood.py), which can be easily adapted to perform equivalent comparisons for other hypothesized water samples and water sources. Figure 4 presents a schematic view of the approach encapsulated by equation (7).

The objective of this study is to determine the likelihood that a given tap water sample originated from a set of possible source waters. We limit the possible location of origin for our tap waters to hydrologic basins west of the continental divide and within the U.S. Within this region, we assign uniform prior values of 1 to these HUC8 regions and a value of zero to all other locations [*Kennedy et al*., 2011]. With the assumption of uniform priors within this region, equation (4) may be simplified and the final likelihood that a specific basin served as the source for a given sample is expressed as the probability that that sample was derived from the location in question, $P(\mathbf{d}_s|\mathbf{d}_l)$, normalized by the maximum value of $P(\mathbf{d}_s|\mathbf{d}_l)$ across all basins within the prior region,

$$\mathcal{L}_r = \frac{P(\mathbf{d}_s|\mathbf{d}_l)}{P(\mathbf{d}_s|\mathbf{d}_l)_{\max}}, \quad (8)$$

where $P(\mathbf{d}_s|\mathbf{d}_l)_{\max}$ is the maximum value of $P(\mathbf{d}_s|\mathbf{d}_l)$ found across all HUC8 regions in the western U.S. This normalization results in a relative likelihood, $\mathcal{L}_r$, ranging from 0 to 1, with a value of 1 denoting the most likely hydrologic basin from which the sample may have been derived. A cutoff threshold of $\mathcal{L}_r = 0.05$ is chosen, below which tap water samples are considered to be isotopically inconsistent with local water resources. This cutoff does not signify that values above 0.05 are guaranteed to be derived from local sources, it only states that we are highly confident that values with $\mathcal{L}_r$ values below 0.05 are derived from nonlocal sources. Finally, we wish to examine the joint likelihood, $\mathcal{L}_r(J)$, that a given HUC8 region uses either local surface water or rainwater for public supply. The value of $\mathcal{L}_r(J)$ is approximated as

$$\mathcal{L}_r(J) = \mathcal{L}_r(RW) + \mathcal{L}_r(SW) - \mathcal{L}_r(RW)\mathcal{L}_r(SW), \quad (9)$$

where the rainwater source likelihood, $\mathcal{L}_r(RW)$, and surface water source likelihood, $\mathcal{L}_r(SW)$, are considered as nonmutually exclusive water supply sources.

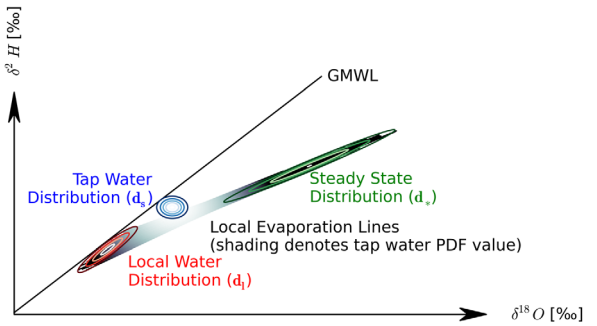

Figure 4. Schematic of likelihood of local origin calculation. The local sample tap water (blue), local water (red), and steady state evaporation (green) composition are characterized by multivariate normal probability distributions. Many random realizations of the local water composition and local steady state composition are used to simulate local evaporation lines (gray lines). These evaporation lines differ in slope from the Global Meteoric Water Line (GMWL), and the line integral of the tap water distribution along these lines is calculated (dark shading on lines) for each realization.

2.3. Modeling Likelihood of Local Water Use

A multivariate regression analysis is used to develop a model for the likelihood of local water resource use for all hydrologic basins in the western U.S. The modeled relative likelihood of local origin, $\hat{\mathcal{L}}_r$, is estimated based on the relative likelihood values, $\mathcal{L}_r$, obtained for all basins with at least five tap water

Table 1. Multivariate Regression Coefficients (β) and Individual Pearson Correlation Coefficients (r) Between Likelihood of Local Origin and Hydrologic Basin Characteristics

HUC8 Hydrologic Basin		Rainfall Source		Surface Source		Joint Source	
Property	Units	β	r	β	r^a	β	r
Latitude	°N	-4.00×10^{-1}	0.12	4.84×10^{-2}	**0.30**	-6.56×10^{-2}	0.27
Longitude	°W	2.86×10^{-1}	0.22	9.95×10^{-2}	−0.04	1.45×10^{-1}	0.07
Area	km^2	1.54×10^{-4}	0.05	-6.12×10^{-5}	0.01	1.96×10^{-5}	0.02
Elevation	m.a.s.l	-9.48×10^{-3}	0.07	-8.65×10^{-4}	−0.18	-2.08×10^{-3}	−0.07
Temperature	°C	$-1.57 \times 10^{+0}$	−0.05	-2.16×10^{-3}	0.06	-2.68×10^{-1}	−0.01
Relative humidity	%	-4.29×10^{-1}	−0.05	-1.92×10^{-2}	0.02	-7.63×10^{-2}	0.01
Rainfall	mm/yr	6.21×10^{-3}	0.21	1.11×10^{-3}	**0.33**	2.47×10^{-3}	***0.34**
Outflow	m^3/yr	1.98×10^{-8}	0.15	-3.53×10^{-9}	0.06	-4.04×10^{-12}	0.14
Population	persons/km^2	2.84×10^{-3}	−0.08	-4.95×10^{-4}	**−0.31**	1.13×10^{-5}	−0.23
Income	$/yr/household	-1.19×10^{-4}	−0.19	-9.15×10^{-6}	***−0.39**	-1.36×10^{-5}	***−0.34**
Available rain water	m^3/person/yr	3.15×10^{-5}	−0.20	-3.36×10^{-6}	0.01	-7.16×10^{-6}	−0.10
Available surface water	m^3/person/yr	1.18×10^{-2}	−0.04	-3.59×10^{-4}	0.21	-1.16×10^{-5}	0.12
Intercept		$9.51 \times 10^{+1}$		$1.01 \times 10^{+1}$		$2.66 \times 10^{+1}$	

[a]Bold correlation coefficients are significant at $p < 0.10$, and * are significant at $p < 0.05$.

samples. When building the models of regional water use patterns, only basins with multiple (≥ 5) samples collected within their watershed are included such that possible variability in supplied tap waters is incorporated. For each such basin, all tap water likelihoods are averaged and compared with hydrologic basin properties (Table 1) including the latitude and longitude of the basin center, area of the basin, average elevation above sea level within the basin, average temperature, average relative humidity, average yearly precipitation falling on the basin, average surface outflow leaving the basin, the population density within the basin, average household income of the families within the basin, available rainwater in the basin (precipitation depth divided by population density), and available surface water in the basin (surface outflow divided by basin area divided by population density).

The modeled multivariate regression value of the likelihood of local origin, $\hat{\mathcal{L}}_r$, is given by

$$\hat{\mathcal{L}}_r = (1 + \exp(-(\beta_0 + \beta_1 z_1 + \ldots + \beta_i z_i)))^{-1}, \quad (10)$$

where z_1 through z_i are the hydrologic basin properties listed above and β_1 through β_i are the regression coefficients, with β_0 the intercept value. The sigmoid form of equation (10) is chosen such that final predicted $\hat{\mathcal{L}}_r$ values are bound between 0 and 1. This approach finds the values of β such that the sum of squared errors between the model result and the normalized likelihoods estimated in section 2.2 is minimized. The standard error of the estimate, $\sigma_{se} = \sqrt{\sum (\mathcal{L}_r - \hat{\mathcal{L}}_r)^2 / N}$, and the r^2 value of the regressions, are used to compare the accuracy of different models.

3. Results

In total, 612 water samples were analyzed spanning the seven western states of Arizona, California, Idaho, Nevada, Oregon, Utah, and Washington. These samples were collected in 199 of the 560 HUC8 regions west of the continental divide in the U.S. (excluding Alaska and Hawaii), with 34 of these regions having at least five samples. Overall, this represents approximately 37% of the total land area and 85% of the population living in the west.

Comparisons between tap water samples and precipitation isotopic composition result in an average likelihood of local origin of 0.10, and reveal limited spatial patterns (Figure 5a). Within the analyzed region, 64% of the tap water samples are inconsistent with the local precipitation isotopic composition, i.e., $\mathcal{L}_r(RW) < 0.05$. Those sites where the likelihood of local precipitation origin are greater than 0.05 cluster primarily in the Pacific north-west, with a set of points in the Seattle-Tacoma region in Washington and the Willamette valley in Oregon having mid-range $\mathcal{L}_r(RW)$ values. Conversely, samples collected from California, Utah, Arizona, Nevada, and western Washington and Oregon fall below the threshold value of 0.05.

Comparisons between tap water samples and surface water isotopic composition reveal much stronger spatial patterns that correspond with many known interbasin water transfer projects (Figure 5b). The average

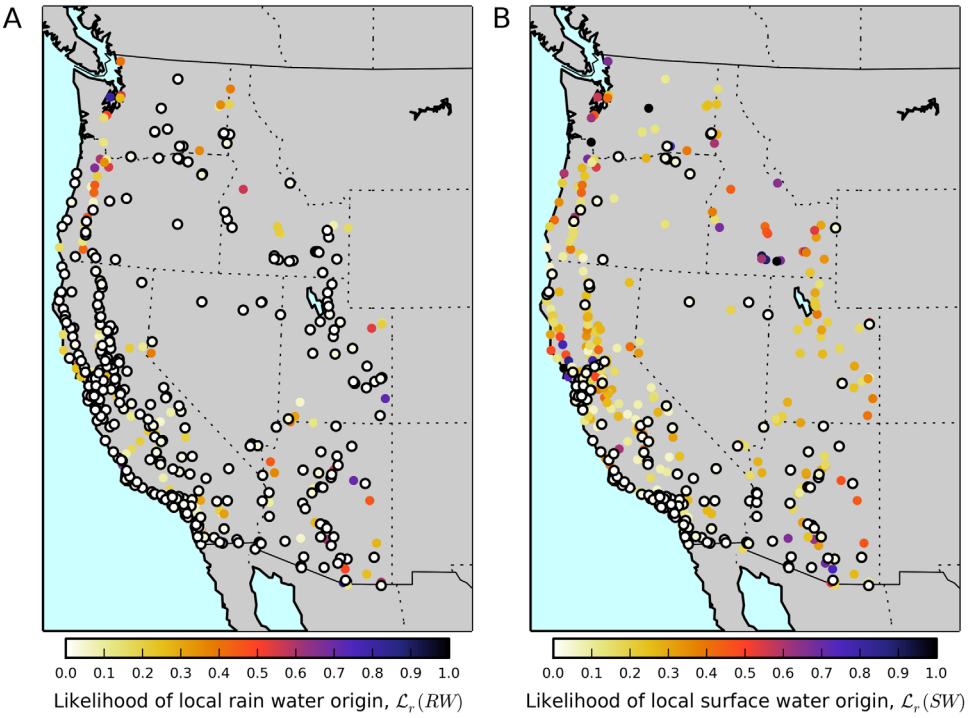

Figure 5. Relative likelihood of local tap water originating from (a) local precipitation and (b) local surface waters. Points with black outlines have an estimated likelihood less than 0.05.

likelihood of local surface water origin is 0.20, and a much lower portion of samples, 31%, is isotopically inconsistent with local surface water sources. Those sites that fall below the 0.05 threshold are primarily clustered in southern California, the San Francisco Bay area, and central Arizona. Isotope values from some locations in the Columbia Plateau of eastern Washington and Oregon, as well as the southern end of California central valley and the California-Oregon border are also inconsistent with local surface waters. The likelihood of local origin obtained assuming a surface water source was consistently higher than likelihood of local origin obtained using an assumed local precipitation source, suggesting that more basins use surface waters than precipitation (e.g., modern groundwater), for public supply.

The joint distribution, those samples that were consistent with either rain or surface values, also exhibits strong spatial pattern similar to that of surface water, yet with consistently higher $\mathcal{L}_r$ values (Figure 6a) as expected from the joint likelihood. In total, only 27% of samples had a joint likelihood that fell below the 0.05 threshold, and the average joint likelihood was 0.27. There is no strong relationship between $\mathcal{L}_r(RW)$ and $\mathcal{L}_r(SW)$, and most points that were below the 0.05 threshold for surface also below the 0.05 threshold for rain waters (Figure 6b). However, multiple points fall below the 0.05 threshold for one of the sources and not the other.

For the estimated local rain and surface waters, 59% and 56%, respectively, of the tap water isotope values were found to be more depleted in the oxygen-18 than local waters. These samples correspond to tap waters that plot to the left and/or below of estimated source water values in δ^{18}O-δ^{2}H space. Isotopic fractionation during evaporation during storage and distribution can only result in enrichment of heavy isotopes (i.e., moving up and to the right in δ^{18}O-δ^{2}H space) and therefore these samples are typically associated with very small $\mathcal{L}_r$ values. However, because of uncertainties and within-basin variability, these relative likelihood estimates are not necessarily zero, especially if tap water samples are only slightly more depleted than local waters.

Across the region, there are stronger relationships between the joint likelihood and basin socioeconomic and hydrogeomorphic characteristics than between likelihood of precipitation or surface origin and these characteristics (Table 1). No statistically significant relationships exist between $\mathcal{L}_r(RW)$ and any of the basin properties. For surface water sources, we find that the basin income (Pearson correlation coefficient

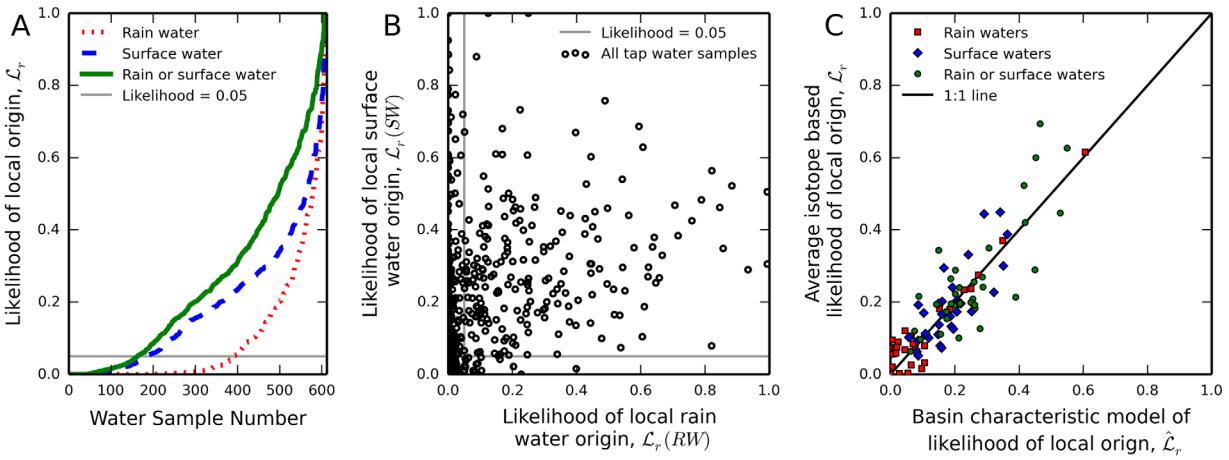

Figure 6. (a) Cumulative distribution of relative likelihoods of local origin for all tap water samples, (b) the relationship between likelihood of rain water origin and likelihood of surface water origin, and (c) hydrogeomorphic and socioeconomic-based modeled likelihoods compared with estimated likelihoods.

$r = -0.39$) is significantly ($p < 0.05$) correlated with $\mathcal{L}_r(SW)$. For the joint source distribution, we find that both basin income ($r = -0.34$) and rainfall ($r = 0.34$) are both significantly correlated with $\mathcal{L}_r(J)$. Overall, higher levels of basin income and population are associated with decreased likelihood of local water use and suggest elevated demand for water resources, while the availability of surface water resources (calculated by dividing basin outflow by population, Figure 7a) determines ability of local water resources to meet this demand.

With the basin hydrogeomorphic and socioeconomic-derived β values (listed in Table 1), we model the likelihood that a hydrologic basin will use locally available surface or rainwater water to supply tap water. The regression for the precipitation source water resulted in a standard error of the estimate of 0.04 and r^2 value of 0.90, while the surface water source regression resulted in a standard error of the estimate of 0.06 and r^2 value of 0.60 (Figure 6c). For the joint likelihood estimate, the standard error of the estimate was 0.09 with an r^2 value of 0.64. Note that interactions between parameters within the multivariate regression can affect the sign of the β coefficients, and because a majority of the $\mathcal{L}_r(RW)$ were near zero, this regression resulted in the highest r^2. Patterns of $\hat{\mathcal{L}}_r(J)$ estimated using the regression model for surface waters are consistent with both the distribution of water availability (Figure 7b) and many known interbasin transfer projects in the west (Figure 1). The multivariate regression model identifies regions such as the Colorado River in northern Arizona and southern Utah, the Columbia River along the Oregon-Washington border, and the Kalmath River in northern California as locations where water importation is least likely. Conversely, the regression model is also able to identify densely populated areas such as San Francisco, Los Angles, and Las Vegas, which import water from beyond their hydrologic basin. The arid Great Basin region of Nevada, southeast Oregon, and western Utah is also identified as an area making use of nonlocal waters.

4. Discussion

Our analysis represents an attempt to evaluate the use of stable H and O isotope ratios to determine environmental sources of water used by humans. Isotopic discrepancies between local waters and collected tap waters are used here to reject the hypothesis that these samples originated from a specific source (local surface or precipitation waters). As discussed in section 1, we would expect that in most, but not necessarily all, of the cases where our analysis rejected a local origin for the tap water denotes importation of water from beyond the local basin or the use of fossil groundwater. However, tap waters isotope values may reflect a number of factors other than those explored here, including desalination sources or as a result of a mixture of multiple source [*Landwehr et al.*, 2013]. Additionally, the possibility exists that waters imported into a basin have an isotopic composition similar to that of local water resources in the basin to which they are transported, as in the case of waters artificially diverted to another HUC8 region down-catchment within

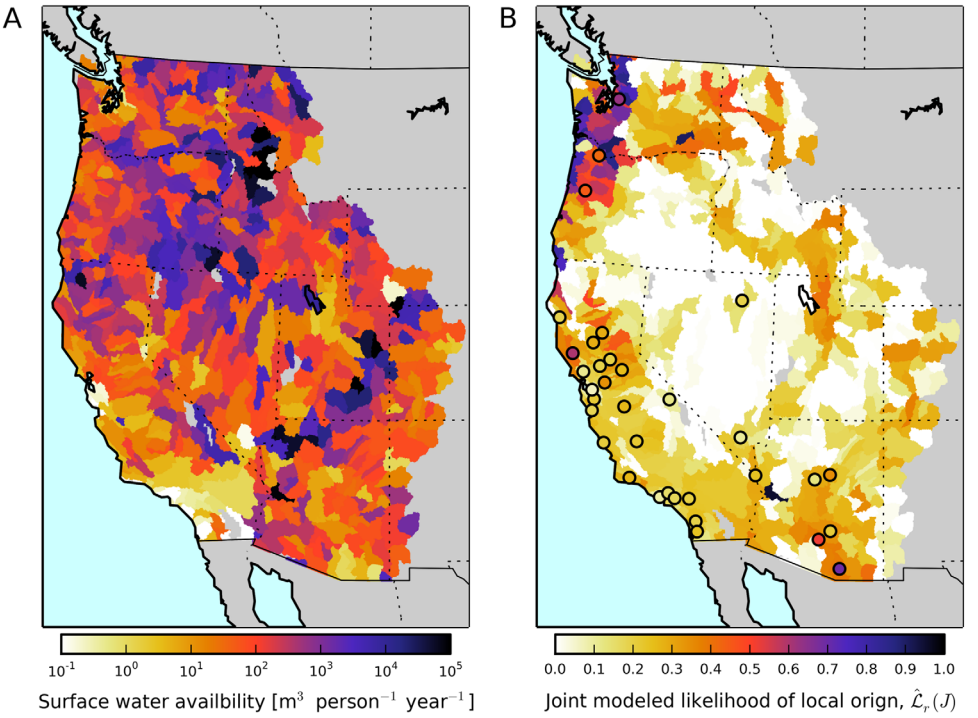

Figure 7. Maps for each HUC8 region of (a) local water availability and (b) hydrogeomorphic and socioeconomic-based modeled likelihood of local surface water use. Colored circles in Figure 7b show the average estimated joint likelihood of local origin for all samples in each basin used for model development and white areas area $\mathcal{L}_r(J) \approx 0$.

the same macrowatershed, and it is unlikely that our analysis would identify all cases of water importation. Nevertheless, most major diversions move water between locations having contrasting hydrogeomorphic (e.g., diversion of high mountain runoff to desert lowland cities) and therefore likely also have difference in their respective isotopic composition. We expect that at the relatively large scale of our analysis, the occurrence of low isotope-based likelihood values is highly correlated with interbasin transfer of water or paleowater use. In the future, more isotope tracers, both light (e.g., $\delta^{17}O$) and heavy (e.g., $^{87}Sr/^{86}Sr$), and informative priors based on hydrogeomorphic and socioeconomic basin parameters may add additional constraints to help resolve these issues and potentially separate imported water from fossil waters.

A comparison of estimated $\mathcal{L}_r$ values based on local precipitation and local surface waters reveals distinct differences. For both precipitation and surface water, amount weighting incorporated in source estimates shifts the expected basin isotopic composition toward those grid cells most likely to possess water resources available in sufficient quantity to be used by local communities. Furthermore, for surface waters, the isotopic contribution of outflow from HUC8 basins upriver also influences regions with significant natural interbasin water movement, such as the basins along the lower Colorado River in Arizona, Nevada, and California. Downstream propagation of water flow is not represented in the precipitation source estimates, which averages values for water falling only on the local HUC8 basin. Inclusion of downstream flow has been previously shown to lead to better agreement between the isotopic values of modeled environmental water sources waters and measured tap waters [*Bowen et al.*, 2011]. An analysis of the discrepancies between the two sets of likelihood estimates derived here demonstrates that in locations where the isotopic difference between precipitation and surface waters is small (such as the Pacific north-west where evaporation is low), the estimated likelihoods also converge. Based on the differences in Figures 5a and 5b, we suggest that isotopic comparison between the joint likelihood of tap water and/or local surface water sources (rather than either precipitation or surface water only) represents the most appropriate approach for identification of cases where water is nonlocal in origin.

When comparing the collected tap water samples to estimates of local water isotopic composition, our method considers the possibility that isotopic differences are due to evaporative enrichment of the heavy

isotopes in the tap water samples. However, there were 359 sites where the tap water samples were more depleted in the heavy isotope than the local rainwater and 340 sites where the tap water was more depleted in the heavy isotope than the local surface water. Such situations could arise either due to inaccuracies in the tap water measurements or source water isotope estimates or as a result of the use of nonlocal water. Because our analysis explicitly considers sources of uncertainty in the sample and source water isotopic values, only 266 of the 359 local rainwater comparisons and 143 of the 340 local surface water comparisons were associated with $\mathcal{L}_r$ values less than 0.05. This demonstrates the robustness of our approach, in that locations where tap waters are more depleted in the heavy isotopes are not necessary assumed to be nonlocal given inherent uncertainties in $\mathbf{d}_l$ and $\mathbf{d}_s$; locations where the tap waters are highly enriched in the heavy isotopes relative to local waters may still be considered local because they fall near the local evaporation line.

As is evident from the estimated and modeled joint local water source likelihoods, tap water samples from coastal California and southern Arizona are isotopically inconsistent with local water resources. This result suggests the importance of major interbasin water transfers for tap water or the mining of fossil groundwater supplies in these regions, which are areas characterized by large water infrastructure projects (Figure 1). Additionally, tap water from locations in the semiarid region east of the Cascade Mountains and central California are isotopically inconsistent with local surface waters. These basins share characteristics with other regions known to import water, in that they receive small yearly rainfall amounts and have high water demand. Groundwater extractions in these regions have lead to significant drops in water levels in both the Central Valley aquifer in California and Columbia Plateau aquifer system west of the Cascade Mountains *Konikow* [2013], and it is possible that sampled tap waters in some of these regions are supplied from fossil groundwater sources. The joint likelihood model identified the Great Basin as an area with a very low likelihood of using local water sources, a finding consistent with previous research that founds significant fossil groundwater use in this arid region [*Smith et al*., 2002].

Though our results are consistent with broad patterns in local and nonlocal water use, our approach is limited by the accuracy and availability of the input precipitation and surface water grids. The previous development of these products [*Bowen and Revenaugh*, 2003; *Bowen et al*., 2011] was predicated on extensive spatiotemporal coverage in sample collections, and the estimates of surface water isotope values are yet to be extended beyond the continental U.S. Additional factors within these products that may lead to inaccuracies in our results. Because the evaporation correction for the surface water model was based on interpolation of model residuals, the surface water model may also overcorrect specific streams, depending on how their hydrology compares to that of other local streams. This may lead to a few sites, where surface water sources appear isotopically heavier than are in reality. Also, those basins situated at higher elevation, such as those east of California's central valley, are likely affected by large quantities of snow pack water storage which complicates the seasonal isotopic signature in surface waters.

Our regression analysis hints at the link between development of major interbasin redistribution projects and economic productivity, with the strongest correlation observed between average income and $\mathcal{L}_r(SW)$. The settlement and development of the western U.S. has long been interwoven with economic activity for multiple reasons, and we do not imply any causation here. Population density is closely linked to income, however, it is not as strong as a predictor possibly due to the high water demand of productive agricultural areas, which may have lower average populations yet high demand and economic output. The estimation of available water within each basin brings together the demand arising from a given population with the potential rainfall or surface water supply; however, the nonsignificant Pearson correlation values for these basin parameters denote additional water resource economic considerations that are not currently captured by our model. A weakly significant latitudinal dependence is also identified ($0.05 < p < 0.10$ for $\mathcal{L}_r(SW)$), and likely arises due to the strong increase in evaporation in southern regions of the western U.S. [*Brown et al*., 2008], as high evaporative losses are expected to increase the need to import waters in these regions. Bringing these predictors together, we are able to model the spatial pattern in local surface water use across the west; however, caution should be applied in directly using these regression values (β's) in other areas of the globe.

Based on an average public supply per capita water use of 99 gallons per day [*Kenny et al*., 2009] and the TIGER census data for each HUC8 region, we calculate the public water supplied to each basin and total

water supplied across the western U.S. at 5.9 billion gallons per day (22 million cubic meters per day). Using the modeled relative likelihood of local water use as an estimate of the fraction of supplied water that is of local origin (i.e., $1-\hat{\mathcal{L}}_r(J)$ approximates the imported fraction), we can develop coarse estimates of interbasin water resource transfers and fossil groundwater extractions across the region. With this approach, we estimate that throughout the western U.S., 4.8 billion gallons per day (17 million cubic meters per day) is moved via interbasin transfers or extracted from nonmodern aquifers. This is equivalent to 1.8 trillion gallons per year (6.2 billion cubic meters per year) and constitutes 81% of the total water supplied in the western U.S., with water importation primarily driven by the large population centers along costal California.

For specific regions known to import large quantities of water, we can compare the isotope-derived water importation volumes with known transfer volumes. The southern California costal region encompassing Los Angles and San Diego (HUC8 18070101–18070305) receives approximately 759 billion gallons of water (2.9 billion cubic meters) per year via the east and west branch of the Los Angles Aqueduct and the Colorado River Aqueduct [*Southern Region Office*, 2009]. The San Francisco Bay region (HUC8 1805001—1805006) receives approximately 411 billion gallons of water (1.6 billion cubic meters) per year via the Mokelumne Aqueduct, Hetch Hetchy Aqueduct, and other smaller projects [*North Central Region Office*, 2009]. For southern California and the San Francisco Bay, we estimate an imported water volume of 573 billon gallons and 212 billion gallons, respectively. These inferred transfer volumes are within a factor of 2 of known values, and are quite accurate given that these estimates are based on isotopic comparisons of tap and local waters (with population information) and do not include any information about water resource infrastructure. The relationship between the true fraction of water imported and the likelihood of local origin merits further investigation in future studies.

As noted in the section 2, equation (5) is given in a general form such that other types of isotopic transformation may be considered. Isotopic offsets occur as local waters are incorporated into plant or animal tissues [*Kelly et al*., 2005; *Ehleringer et al*., 2008]. Similarly, various commercial processes such as the production of beers and wines are associated with isotopic fractionation [*Chesson et al*., 2010]. If the form of these processes can be modeled, new $g(t)$ functions can be specified and likelihoods of other types of samples being derived from any specific, isotopically characterized, sources can be assessed. Thus, this methodology provides a unique quantitative approach to isotopic investigations into studies of provenance.

5. Conclusions

In this study, we present an investigation into the origin of tap water based on isotopic comparison between collected samples and modeled local water resources. Using a database of 612 tap waters from the western U.S., we demonstrate that tap waters from many areas known to import water from beyond their local hydrologic basin have an isotopic composition that is inconsistent with local waters. These results are derived using a new method that accounts for uncertainty in the sample and source water isotopic compositions and the possibility of evaporative enrichment during storage and distribution of water. Based on our analysis, we find that tap waters are in most cases isotopically distinct from local, basin-average, precipitation, whereas the majority of tap waters are isotopically similar to surface water resources available in the local basin. Most locations where the isotopic composition of supplied water is inconsistent with that of local surface waters are clustered in distinct regions of the western U.S. and are likely importing waters from beyond their watershed.

Regional patterns in the isotopically estimated likelihood that supplied waters are of local origin demonstrate that interbasin water transfers or fossil groundwater extraction occurs primarily in basins with stronger economic activity and limited surface water availability. Interbasin transfer projects and paleowater withdrawals are a critical component of western water resource infrastructure, and based on our modeled likelihoods we estimate nonlocaly sourced waters are supplied to approximately 36 million people via 4.8 billon gallons of transferred water per day. The approach presented here not only provides a new tool for assessing patterns of water resource transfer within the U.S., but is also applicable worldwide, where direct collection of supplied waters could provide a global perspective on interbasin water transfers.

Acknowledgments
Partial funding for this work was provided by the U.S. Federal Government and U.S. National Science Foundation grant EF-01241286 to G.J.B. M. Beasley acknowledges the assistance of Andrew Somerville, Kathleen Beasley, Jillian Johnson, and Nicole Barger in collection of samples.

References

Beasley, M. M., L. A. Chesson, L. O. Valenzuela, and E. J. Bartelink (2013), Extending the biological profile: Using stable isotope analysis as an exclusionary tool in region-of-origin investigations of unidentified remains, *Proc. Am. Acad. Forensic Sci.*, *19*, 470.

Bowen, G., and J. Revenaugh (2003), Interpolating the isotopic composition of modern meteoric precipitation, *Water Resour. Res.*, *39*(10), 1299, doi:10.1029/2003WR002086.

Bowen, G., J. Ehleringer, L. Chesson, E. Stange, and T. Cerling (2007), Stable isotope ratios of tap water in the contiguous united states, *Water Resour. Res.*, *43*, W03419, doi:10.1029/2006WR005186.

Bowen, G., C. Kennedy, Z. Liu, and J. Stalker (2011), Water balance model for mean annual hydrogen and oxygen isotope distributions in surface waters of the contiguous United States, *J. Geophys. Res.*, *116*, G04011, doi:10.1029/2010JG001581.

Bowen, G. J., and B. Wilkinson (2002), Spatial distribution of δ^{18}O in meteoric precipitation, *Geology*, *30*(4), 315–318.

Bowen, G. J., C. D. Kennedy, P. D. Henne, and T. Zhang (2012), Footprint of recycled water subsidies downwind of lake Michigan, *Ecosphere*, *3*(6), 1–16.

Brown, D., J. Worden, and D. Noone (2013), Characteristics of tropical and subtropical atmospheric moistening derived from Lagrangian mass balance constrained by measurements of HDO and H_2O, *J. Geophys. Res. Atmos.*, *118*, 54–72, doi:10.1029/2012JD018507.

Brown, T. C., M. T. Hobbins, and J. A. Ramirez (2008), Spatial distribution of water supply in the coterminous United States, *J. Am. Water Resour. Assoc.*, *44*(6), 1474–1487.

Buckley, J. (2013), Quantifying the impacts of interbasin transfers on water balances in the conterminous United States, MS thesis, N. C. State Univ., Raleigh.

Census (2013), *TIGER/Line Shapefiles*, U.S. Census Bur., Washington, D. C.

Chesson, L. A., L. O. Valenzuela, S. P. O'Grady, T. E. Cerling, and J. R. Ehleringer (2010), Links between purchase location and stable isotope ratios of bottled water, soda, and beer in the United States, *J. Agric. Food Chem.*, *58*(12), 7311–7316.

Cooley, H., and K. Donnelly (2012), Proposed seawater desalination facilities in California, technical report, Pac. Inst., Oakland, Calif. [Available at http://pacinst.org/publication/key-issues-in-seawater-desalination-proposed-facilities/.]

Coplen, T. B. (1996), New guidelines for reporting stable hydrogen, carbon, and oxygen isotope-ratio data, *Geochim. Cosmochim. Acta*, *60*(17), 3359–3360.

Coplen, T. B. (2011), Guidelines and recommended terms for expression of stable-isotope-ratio and gas-ratio measurement results, *Rapid Commun. Mass Spectrom.*, *25*(17), 2538–2560.

Craig, H. (1961), Isotopic variations in meteoric waters, *Science*, *133*(3465), 1702–1703.

Daly, C., W. P. Gibson, G. H. Taylor, G. L. Johnson, and P. Pasteris (2002), A knowledge-based approach to the statistical mapping of climate, *Clim. Res.*, *22*(2), 99–113.

Dansgaard, W. (1964), Stable isotopes in precipitation, *Tellus*, *16*(4), 436–468.

De Laeter, J., J. Böhlke, P. De Biévre, H. Hidaka, H. Peiser, K. Rosman, and P. Taylor (2003), Atomic weights of the elements: Review 2000, *Pure Appl. Chem.*, *75*(6), 683–800.

Draper, A. J., M. W. Jenkins, K. W. Kirby, J. R. Lund, and R. E. Howitt (2003), Economic-engineering optimization for California water management, *J. Water Resour. Plann. Manage.*, *129*(3), 155–164.

Ehleringer, J. R., G. J. Bowen, L. A. Chesson, A. G. West, D. W. Podlesak, and T. E. Cerling (2008), Hydrogen and oxygen isotope ratios in human hair are related to geography, *Proc. Natl. Acad. Sci. U.S.A.*, *105*(8), 2788–2793.

Fort, D., B. Nelson, K. Coplin, and S. Wirth (2012), *Pipe Dreams: Water Supply Pipeline Projects in the West*, Natl. Resour. Def. Counc., Washington, D. C.

Gat, J. (1996), Oxygen and hydrogen isotopes in the hydrologic cycle, *Ann. Rev. Earth Planet. Sci.*, *24*(1), 225–262.

Gat, J., and Y. Levy (1978), Isotope hydrology of inland Sabkhas in the Bardawil area, Sinai, *Limnol. Oceanogr.*, *23*(5), 841–850.

Gedzelman, S. D., and J. R. Lawrence (1990), The isotopic composition of precipitation from two extratropical cyclones, *Mon. Weather Rev.*, *118*(2), 495–509.

Ghassemi, F., and I. White (2007), *Inter-Basin Water Transfer: Case Studies From Australia, United States, Canada, China and India*, Cambridge Univ. Press, Cambridge, U. K.

Gibson, J., and T. Edwards (2002), Regional water balance trends and evaporation–transpiration partitioning from a stable isotope survey of lakes in northern Canada, *Global Biogeochem. Cycles*, *16*(2), doi:10.1029/2001GB001839.

Gibson, J., S. Birks, and T. Edwards (2008), Global prediction of δ_A and δ^2H-δ^{18}O evaporation slopes for lakes and soil water accounting for seasonality, *Global Biogeochem. Cycles*, *22*, GB2031, doi:10.1029/2007GB002997.

Good, S. P., D. V. Mallia, J. C. Lin, and G. J. Bowen (2014), Stable isotope analysis of precipitation samples obtained via crowdsourcing reveals the spatiotemporal evolution of superstorm sandy, *PLoS ONE*, *9*(3), 1–7, doi:10.1371/journal.pone.0091117.

Grant, E. H. C., H. J. Lynch, R. Muneepeerakul, M. Arunachalam, I. Rodríguez-Iturbe, and W. F. Fagan (2012), Interbasin water transfer, riverine connectivity, and spatial controls on fish biodiversity, *PLoS ONE*, *7*(3), e34170.

Gupta, J., and P. van der Zaag (2008), Interbasin water transfers and integrated water resources management: Where engineering, science and politics interlock, *Phys. Chem. Earth*, *33*(1), 28–40.

Jenkins, M. W., J. R. Lund, R. E. Howitt, A. J. Draper, S. M. Msangi, S. K. Tanaka, R. S. Ritzema, and G. F. Marques (2004), Optimization of California's water supply system: Results and insights, *J. Water Resour. Plann. Manage.*, *130*(4), 271–280.

Kelly, S., K. Heaton, and J. Hoogewerff (2005), Tracing the geographical origin of food: The application of multi-element and multi-isotope analysis, *Trends Food Sci. Technol.*, *16*(12), 555–567.

Kendall, C., and T. Coplen (2001), Distribution of oxygen-18 and deuterium in river waters across the United States, *Hydrol. Processes*, *15*(7), 1363–1393.

Kennedy, C. D., G. J. Bowen, and J. R. Ehleringer (2011), Temporal variation of oxygen isotope ratios (δ^{18}O) in drinking water: Implications for specifying location of origin with human scalp hair, *Forensic Sci. Int.*, *208*(1), 156–166.

Kenny, J. F., N. L. Barber, S. S. Hutson, K. S. Linsey, J. K. Lovelace, and M. A. Maupin (2009), Estimated use of water in the United States in 2005, *U.S. Geol. Surv. Circ. 1344*, 52 pp.

Konikow, L. F. (2013), Groundwater depletion in the United States (1900–2008), *U.S. Geol. Surv. Sci. Invest. Rep., 2013–5079*, 63 pp.

Konikow, L. F., and E. Kendy (2005), Groundwater depletion: A global problem, *Hydrogeol. J.*, *13*(1), 317–320.

Landwehr, J. M., T. B. Coplen, and D. W. Stewart (2013), Spatial, seasonal, and source variability in the stable oxygen and hydrogen isotopic composition of tap waters throughout the USA, *Hydrol. Processes*, *28*, 5382–5422, doi:10.1002/hyp.10004.

Lynch, H. J., E. H. Campbell Grant, R. Muneepeerakul, M. Arunachalam, I. Rodriguez-Iturbe, and W. F. Fagan (2011), How restructuring river connectivity changes freshwater fish biodiversity and biogeography, *Water Resour. Res.*, *47*, W05531, doi:10.1029/2010WR010330.

Mooty, W., and H. Jeffcoat (1986), Inventory of interbasin transfers of water in the western conterminous United States, *U.S. Geol. Surv. Tech. Rep. 86–148*, 53 pp.
North Central Region Office (2009), *California Water Plan, Update 2009, vol. 3, Regional Reports: San Fransisco Bay*, Dep. of Water Resour., Sacramento, Calif.
Petsch, H. E. (1985), Inventory of interbasin transfers of water in the western conterminous United States, *U.S. Geol. Surv. Tech. Rep. 85–166*, 45 pp.
Rozanski, K., L. Araguás-Araguás, and R. Gonfiantini (1993), Isotopic patterns in modern global precipitation, *Geophys. Monogr. Ser.*, *78*, 1–36.
Seirup, L., and G. Yetman (2006), U.S. census grids (summary file 3), 2000, NASA Socioecon. Data and Appl. Cent., Palisades, N. Y. [Available at http://sedac.ciesin.columbia.edu/data/set/usgrid-summary-file3-2000.]
Smith, G. I., I. Friedman, G. Veronda, and C. A. Johnson (2002), Stable isotope compositions of waters in the great basin, United States: 3. Comparison of groundwaters with modern precipitation, *J. Geophys. Res.*, *107*(D19), 4402, doi:10.1029/2001JD000567.
Soderberg, K., S. P. Good, M. O'Conner, L. Wang, K. Ryan, and K. K. Caylor (2013), Using atmospheric trajectories to model the isotopic composition of rainfall in central Kenya, *Ecosphere*, *4*(3):33, 1–18, doi:10.1890/ES12-00160.1.
Southern Region Office (2009), *California Water Plan, Update 2009, vol. 3, Regional Reports: South Coast*, Dep. of Water Resour., Glendale, Calif.
Sultan, M., E. Yan, N. Sturchio, A. Wagdy, K. Abdel Gelil, R. Becker, N. Manocha, and A. Milewski (2007), Natural discharge: A key to sustainable utilization of fossil groundwater, *J. Hydrol.*, *335*(1), 25–36.
USGS (2013), *Federal Standards and Procedures for the National Watershed Boundary Dataset (WBD) Techniques and Methods 11-A3*, 4th ed., U.S. Geol. Surv. and U.S. Dep. of Agric. Natl. Resour. Conserv. Serv., Reston, Va.
Vachon, R., J. Welker, J. White, and B. Vaughn (2010), Monthly precipitation isoscapes ($\delta^{18}O$) of the United States: Connections with surface temperatures, moisture source conditions, and air mass trajectories, *J. Geophys. Res.*, *115*, D21126, doi:10.1029/2010JD014105.
Vörösmarty, C. J., et al. (2010), Global threats to human water security and river biodiversity, *Nature*, *467*(7315), 555–561.
Williams, A. E., and D. P. Rodoni (1997), Regional isotope effects and application to hydrologic investigations in southwestern California, *Water Resour. Res.*, *33*(7), 1721–1729.
Wu, C.-F. J. (1986), Jackknife, bootstrap and other resampling methods in regression analysis, *Ann. Stat.*, *14*(4), 1261–1295.
Wunder, M. B. (2010), Using isoscapes to model probability surfaces for determining geographic origins, in *Isoscapes*, pp. 251–270, Springer, Dordrecht, Netherlands.
Wunder, M. B., C. L. Kester, F. L. Knopf, and R. O. Rye (2005), A test of geographic assignment using isotope tracers in feathers of known origin, *Oecologia*, *144*(4), 607–617.
Yan, D., H. Wang, H. Li, G. Wang, T. Qin, D. Wang, and L. Wang (2012), Quantitative analysis on the environmental impact of large-scale water transfer project on water resource area in a changing environment, *Hydrol. Earth Syst. Sci.*, *16*(8), 2685–2702.